Conductivity Anomalies around the Izu-Bonin Arc-Trench System

H. Toh and J. Segawa

Ocean Research Institute, The University of Tokyo

Abstract: Since 1986 we have been carrying out seafloor geomagnetic and geoelectric observations around the northern Izu-Bonin arc-trench system. In 1989 the observation was focused on the comparative study on both sides of the trench, the results of which was summarized in the following: (1) One dimensional (1D) analysis of the magnetotelluric (MT) data observed on the Pacific plate shows that the depth to the asthenospheric conductor should be around 150 km. (2) The calculated geomagnetic transfer functions have northward components in shorter periods (e.g., shorter than 30 min) while they tend to point toward south in longer periods (e.g., longer than 60 min).

1. Introduction

The reason why we have been operating sea floor geomagnetic and geoelectric observations around the Izu-Bonin arc is to construct a model of electrical conductivity structure beneath the arc, which will lead to the general understanding of the origin, evolution and present structure of the typical island arc system if it is interpreted together with other geophysical data. Some features have been revealed by the observations conducted so far, and we qualitatively summarize them by mapping induction vectors as shown by Fig. 1. Although the induction vectors of the southernmost observation line show an almost 2D structure of the Izu-Bonin arc, those of the northernmost observation line seem to be definitely affected by the Japan arc. It implies that the conductivity anomalies around this area consist of those originated from the Izu-Bonin arc itself and those from the Japan arc. We think it is meaningful to estimate a 2D conductivity structure of the Izu-Bonin arc first as an initial model in order to construct a final three dimensional (3D) conductivity model around the region.

A 2D modelling of a conductivity structure requires boundary conditions at both infinities. For this purpose, an MT method is more preferable than a geomagnetic deep sounding (GDS) method because oceanic

basins are, to first approximation, considered to have stratified structures. Utada (1987) estimated the depth to the upper mantle conductor beneath the Shikoku basin as about 30 km through the sea floor MT observations around the Philippine sea, but there is no data available on the Pacific plate side except for one site off Tohoku District (Yukutake et al., 1983). This is the main reason why we made the MT observation at the sea floor across the trench in 1989. In addition, geomagnetic observation sites were set on the other side of the trench to make a comparison with the MT site in the 1989 experiment.

2.Instrumentation

In 1989 five instruments were installed at four sites. They consisted of three fluxgate type three-component ocean bottom magnetometers (OBM's), one two-component ocean bottom electrometer (OBE) and one ocean bottom electromagnetometer (OBEM). OBEM can measure two electric components and three geomagnetic components simultaneously. OBE and one of OBM's (OBM-S4) were installed at the same site (JK20) for MT measurement. Each OBM, OBE and OBEM was equipped with a beacon, a flasher and an acoustic release system.

Figure 2 and 3 show the outer view of OBM-S4 and OBE, respectively. These two instruments were deployed at depths larger than 5000 m. The lack of data on the Pacific plate side was mostly because it was too deep for the usual pressure tight vessels. Therefore, the pressure tight glass spheres for these two instruments were replaced by either an aluminum sphere (for OBM-S4) or a titanium cylinder (for OBE).

Here, we make some comments on the ocean bottom electrometer (OBE) because it is new in practical use compared with the ocean bottom magnetometers. Hamano (personal communication, 1985) showed that a pair of sintered silver-silverchloride electrodes is effective for the sea floor electric field measurement because of the small drift rate and small contact potential difference in seawater. Making use of this kind of electrodes, we also succeeded in ocean bottom electric field observation in 1987. This time, these electrodes were used for OBE as well. Long span electrodes are preferable in terms of low signal to noise ratio of electric fields at the sea floor, but it is impossible to extend the span longer than 10 m for the sake of on-board operation of the instrument. A 5 m span is usually adopted and

considered to be long enough for practical electric field measurement at the sea floor as is the case of this experiment.

3.Observation and Data

The installation of instruments in the 1989 experiment was mainly made on the east-west (EW) transverse section of the Izu-Bonin arc at 32°N. It took about three days to complete installation. Figure 4 shows the location of the installation points on a bathymetric chart together with the past observation points. The key stations of the experiment lie on either side of the trench. OBEM, OBE and OBM-S4 were installed to the east of the trench for MT sounding of the Pacific plate. The other two OBM's were distributed on the fore arc for a comparison with the geomagnetic measurement on the Pacific plate.

The recovery of the instruments was all successfully made by the Umitaka-maru, Tokyo University of Fisheries, from 16th/SEP/'89 to 19th/SEP/'89. Unfortunately, OBEM did not work well, but the rest of the instruments gave sufficient and good quality geomagnetic and geoelectric variational data at the sea floor. Figure 5 through 7 show sample plots of geomagnetic three components obtained from the instrument OBM-S4 at site JK20, horizontal geoelectric two components from OBE at the same site JK20 and geomagnetic three components from OBM-S5 at site JK21. Geomagnetic storms observed in the geoelectric and geomagnetic time series were analyzed by a fast Fourier transform method assuming the time dependence of $e^{+i\omega t}$, from which both geomagnetic transfer functions and MT parameter estimates were obtained.

As for more detailed information of installation sites and data, refer to Table 1.

4.Results

In this section, we first describe the MT results on the Pacific plate and bring forward an optimum 1D model of the oceanic plate.

Second, we show the GDS results by adding those of the 1989 experiment to our previous results in this area.

4.1.1D MT modelling

Table 1 Observation Log of KH89-1 Cruise

Apparatus	Site	Position	Depth	Duration	Sampling Rate
OBEM	JK19	32°22.1'N 144°11.0'E	5431m	-	1 min.
OBE	JK20	31°59.8'N 143° 0.1'E	5685m	83 days	1 min.
OBM-S4	JK20	31°59.6'N 140°59.9'E	5696m	83 days	2 min.
OBM-S5	JK21	32° 0.0'N 140°59.9'E	2703m	82 days	2 min.
OBM-C3	JK22	33° 0.1'N 140°30.1'E	1218m	81.5 days	2 min.

Utada (1987) derived the most reliable conductivity models for both central Japan and for northeast Japan using a non-linear 2D inversion technique. According to his model, the conductivity structure beneath the ocean has the following features:

(1) The depth to the asthenospheric conductor d_A differs between below the Shikoku basin and below the Pacific plate, i.e., $d_A \approx 30$ km for the Shikoku basin and 150 km for the Pacific plate.

(2) Thin conducting layers (TCL's) appear at the top of the two oceanic plates.

Although TCL's seem to certainly exist, the thicknesses are still unknown because of the lack of high frequency signals at the sea floor. We, however, determined d_A of the Pacific plate in the east of the Izu-Bonin arc by 1D MT modelling assuming the conductivity of TCL as 0.1 S/m and thickness 10 km, i.e., the net conductance of TCL = 1000 S.

In the modelling, we took another fixed parameter, i.e., the conductivity of the resistive oceanic plate, as 0.002 S/m, while the thickness of the resistive layer ($\approx d_A$) and the conductivity of the infinite half space σ_A were varied. Two models are presented here for comparison. One is model A whose d_A and σ_A are 30 km and 0.1 S/m, respectively. Model A can be compared to the actual Shikoku basin. Another model B is characterized by d_A = 150 km and σ_A = 1 S/m.

Figures 8(a) and 8(b) show the result for model A and model B, respectively. Model A can explain neither amplitude nor phase, whereas much progress is seen in model B. We took σ_A = 1 S/m , not 0.1 S/m, in order to improve the accordance of the calculated phases with the observed phases.

4.2.Transfer functions

Figures 9(a) through 9(d) show the induction vectors for the period of 15 min (a), 30 min (b), 60 min (c) and 120 min (d) in this area. The characteristics of the induction vectors are described as follows:

(1) In shorter periods (e.g., shorter than 30 min), the calculated induction vectors have northward components especially for the northern two profiles which lie on 33°N and 32°N.

(2) In longer periods (e.g., longer than 60 min), the vectors change their direction to the south.

The former is the most remarkable result of the 1989 experiment. Induced electric currents in the ocean are thought to be strongly concentrated and flow along the trench. If it is true, the induction vectors at JK20 and JK21 point toward the trench axis and they have opposite directions each other. The observed vectors, however, have northward components, which implies that the induced currents flow along EW direction rather than north-south (NS) direction.

The latter is also very suggestive. The change of the direction of the vectors occurs between the period of 30 min and 60 min, which implies the existence of some deeper anomalies.

5.Summary and Concluding Remarks

The improvement of the pressure tight vessels of the instruments as well as practical usage of OBE have made it possible to carry out both MT and GDS measurement in the deep northwestern Pacific region. The 1D MT sounding of the Pacific plate reveals that the depth to the asthenospheric conductor is also around 150 km east of the Izu-Bonin trench, which is in agreement with the result of Utada (1987). We think it imposes constraint on the 2D conductivity modelling of the Izu-Bonin arc.

The observed transfer functions show a 3D distribution rather than 2D, especially for the northernmost EW profile. The short-period (shorter than 30 min) induction vectors along the profile point to the north, suggesting the existence of current leakage from the Pacific ocean into the Philippine sea (and vice-versa) via the north end of the arc. However, the effect of shallower structure, i.e., local bathymetry and/or the distribution of

sedimentary layers should be estimated by some direct observations or theoretical studies before considering it to be responsible for the conduction effect. The long-period (longer than 60 min) vectors of all the 3 profiles point to the south suggesting a deep structure produced by the interaction of the Japan arc and the Izu-Bonin arc. A deep structure, however, would become ambiguous without a well defined shallow structure. This is also the reason why it is desirable that some direct electromagnetic observations of shallow structures beneath the ocean, using such as the controlled source methods, is applied to practical use.

Acknowledgements

We are grateful to all the crew on the Hakuho-maru for their kind cooperation in installation. We also wish to express our sincere thanks to the crew of the Umitaka-maru, Tokyo University of Fisheries, for their helpful assistance in the recovery of the instruments.

REFERENCES

Utada, H., A direct inversion method for two-dimensional modeling in the geomagnetic induction problem, Ph. D. Thesis, Univ. of Tokyo, 1987

Yukutake, T., J. H. Filloux, J. Segawa, Y. Hamano and H. Utada, Preliminary report on a magnetotelluric array study in the northwest Pacific, J. Geomag. Geoelectr., 35, 575-587, 1983

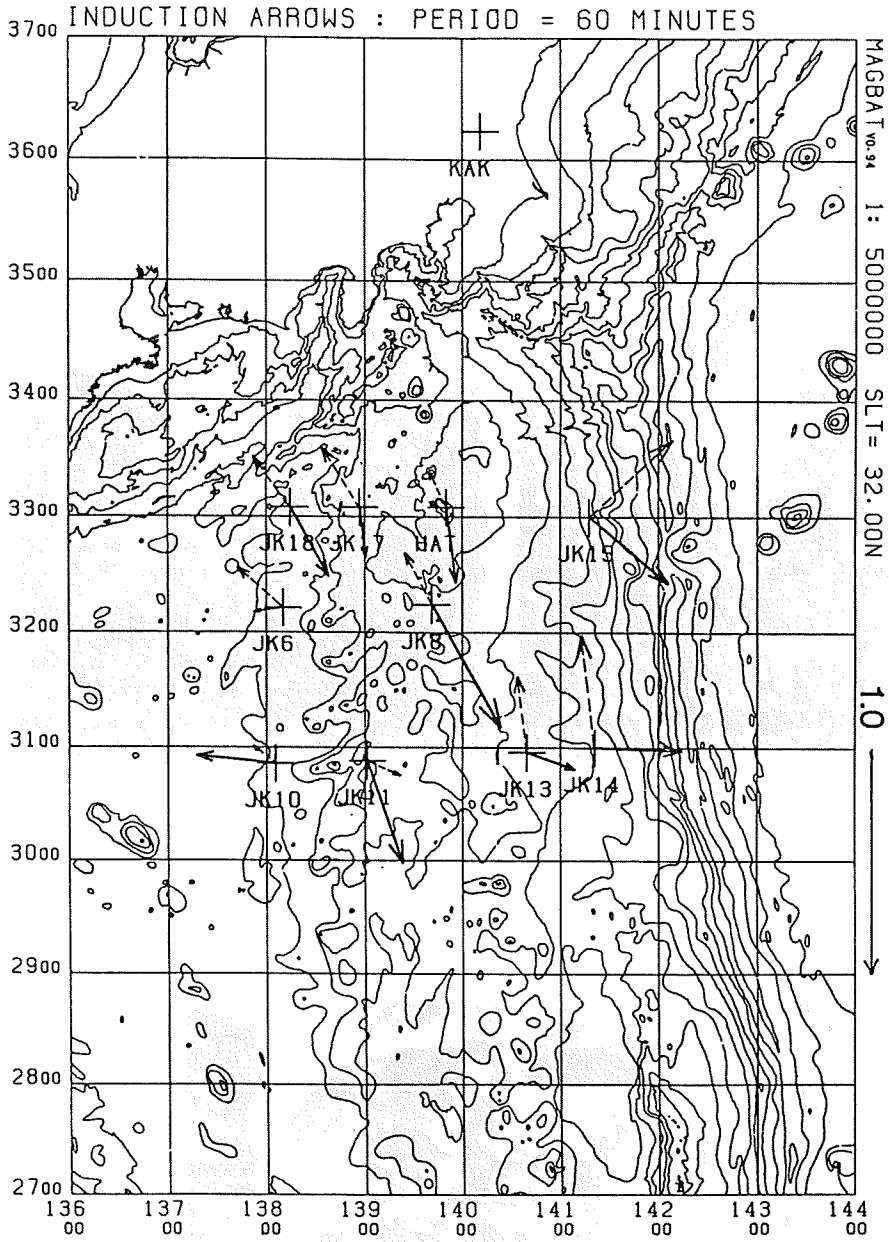

Fig. 1 Mapping of the induction vectors in the vicinity of the Izu-Bonin arc for the period of 60 minutes. Solid arrows indicate the real parts of the calculated transfer functions, while dashed arrows denote imaginary. The unit length for the arrows is also shown outside the grid.

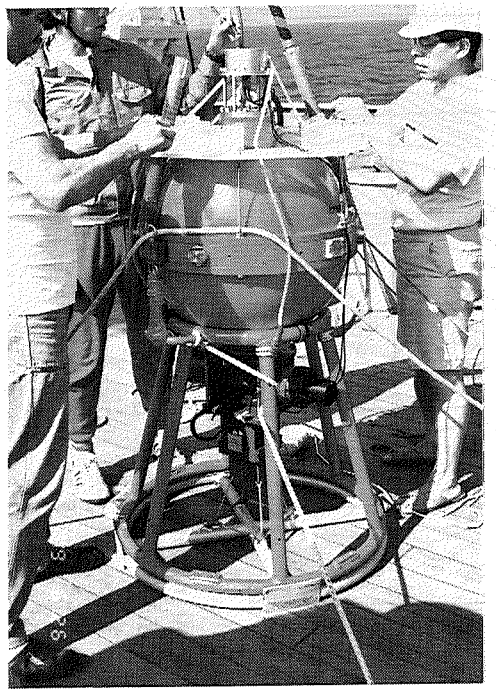

Fig. 2 A photograph of OBM-S4 on board just before launch.

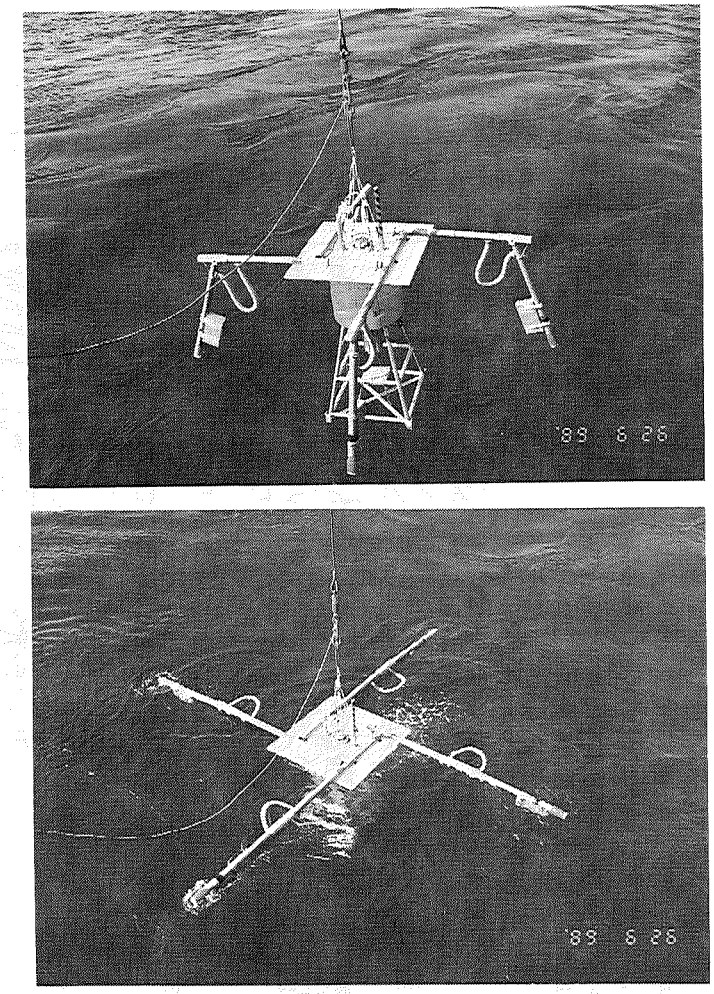

Fig. 3 Photographs of OBE at the sea surface showing the performance of the arm extension in seawater.

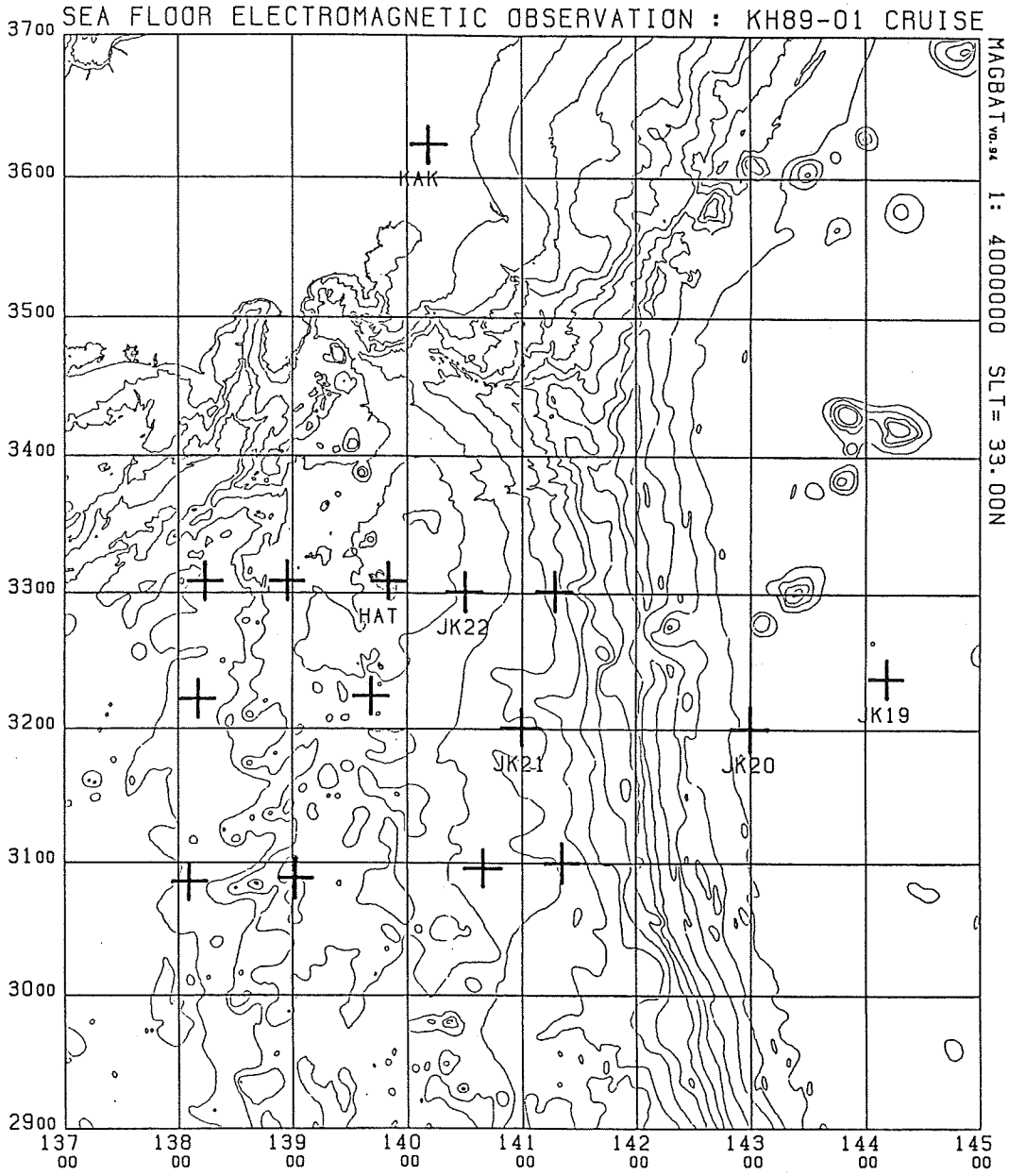

Fig. 4 A map of observation sites. JK19 through JK22 show the positions of the observation sites in the 1989 experiment. Cross marks without site names represent the previous observation sites in this area. The locations of Kakioka (KAK) and Hachijo-jima (HAT) are also shown.

Fig. 5 A sample plot of geomagnetic variations at site JK20 from 14th/AUG/'89 00:00 JST to 17th/AUG/'89 23:59 JST. Three solid lines correspond to geomagnetic north(H), geomagnetic east(D) and downward(Z) components from top to bottom, respectively. One division of the vertical axis is 40 nT.

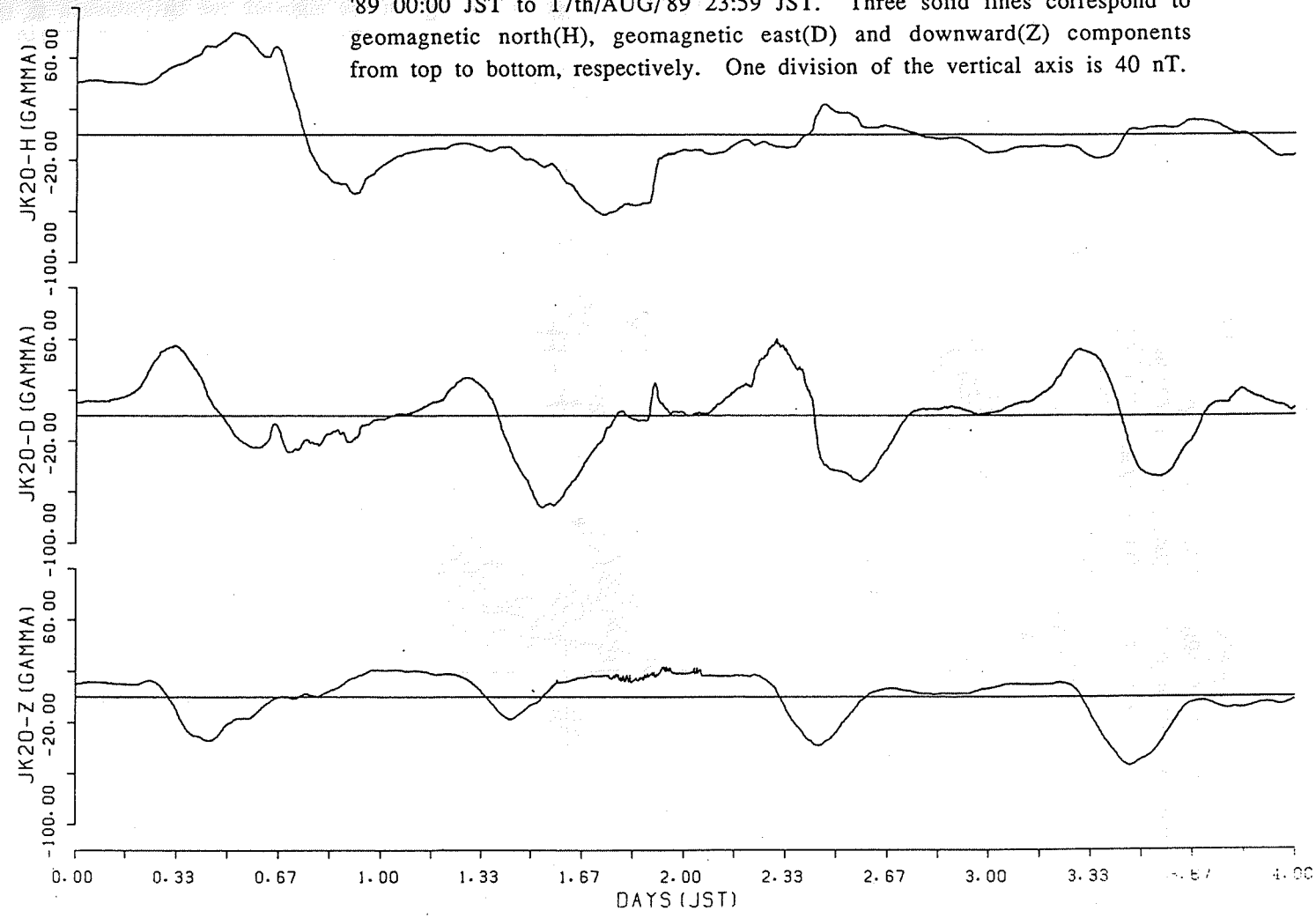

Fig. 6 A simultaneous plot of horizontal geoelectric variations with Fig. 5 at the same site JK20. Ex (upper) and Ey (lower) component are shown. They are measured along geomagnetic north and geomagnetic east, respectively. One division of the vertical axis is about 3 μV/m.

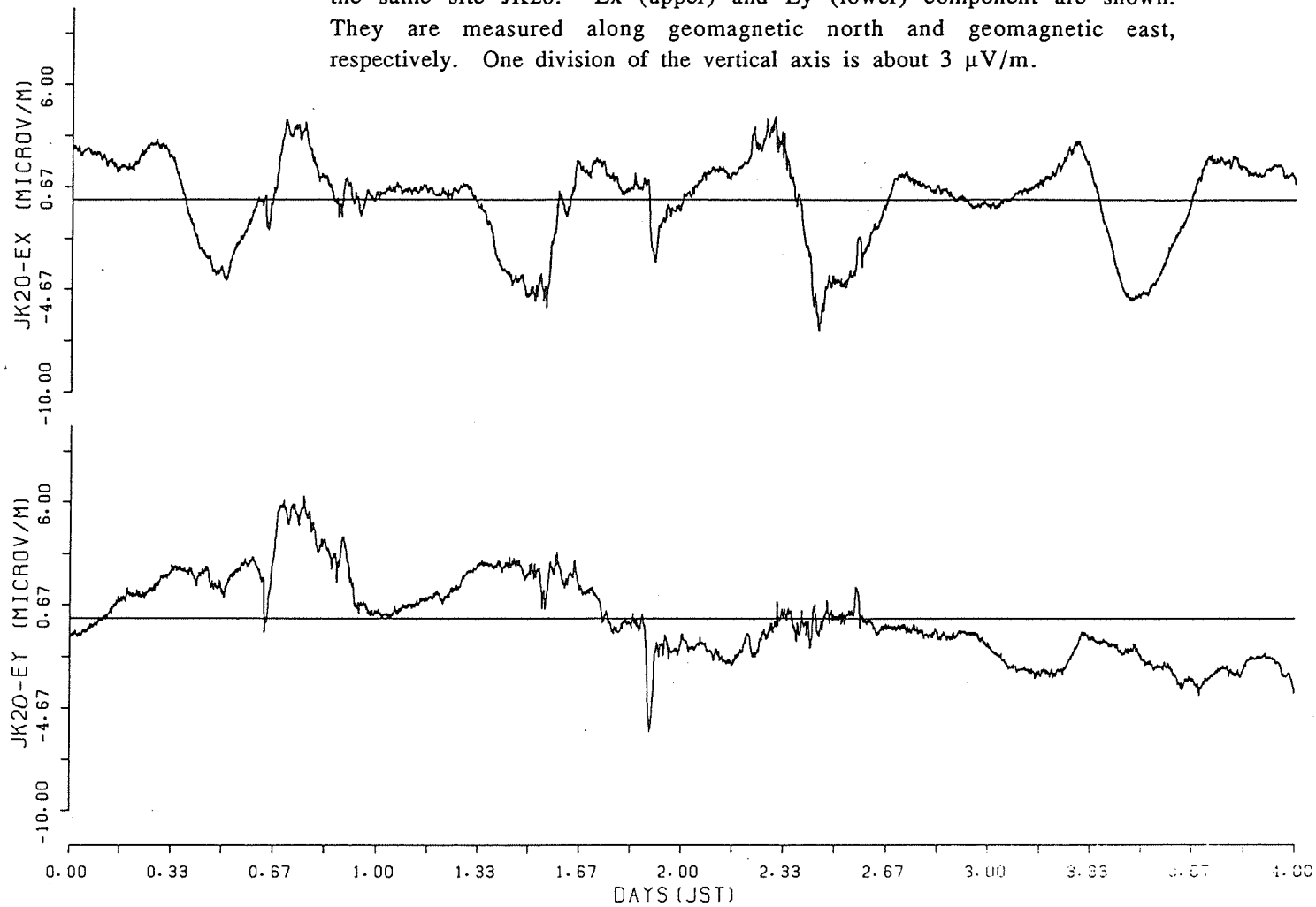

Fig. 7 A simultaneous plot of geomagnetic variations with Fig. 5 at site JK21. Axes and components are the same as Fig. 5.

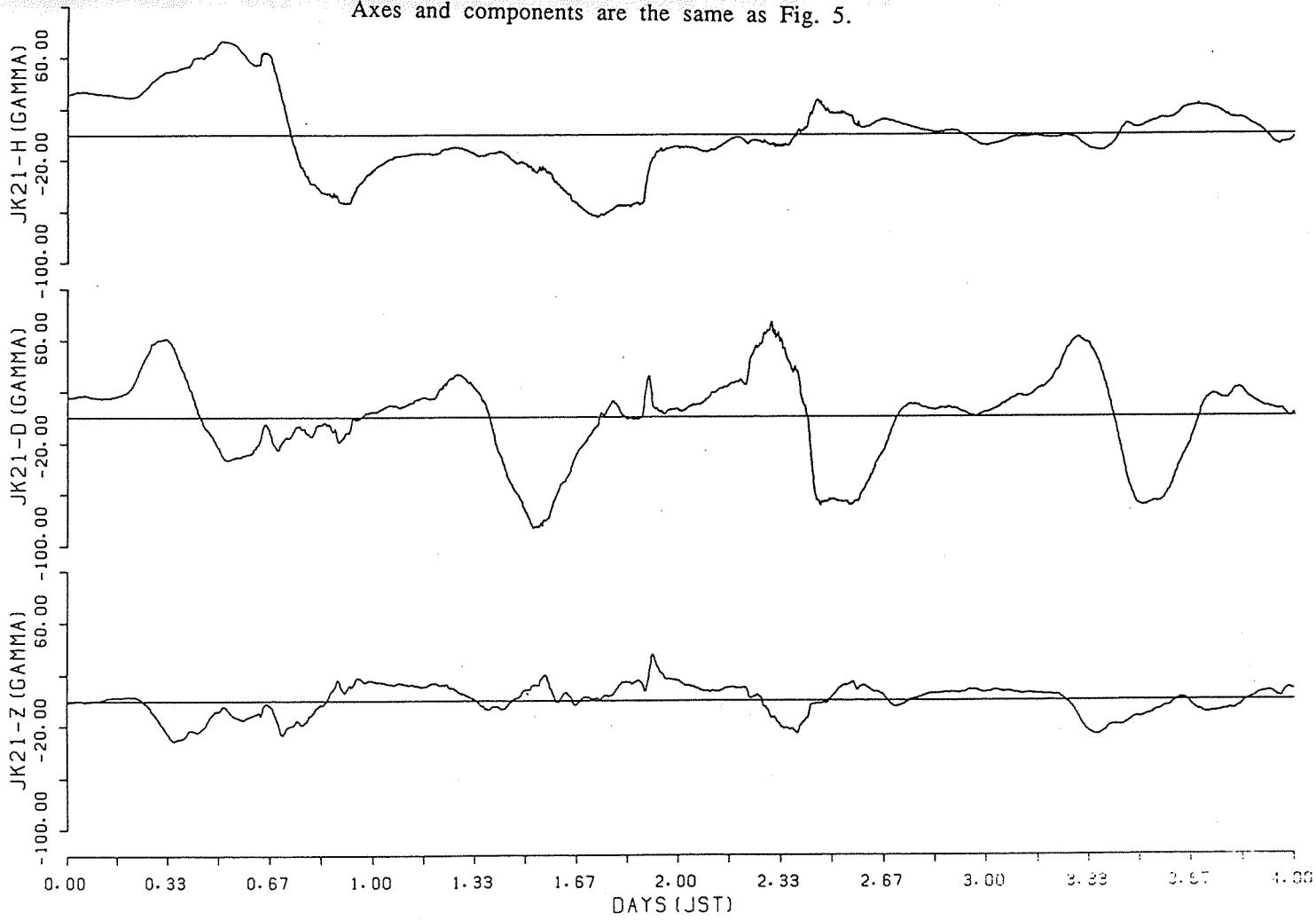

Fig. 8(a), (b) Apparent resistivity (upper) and its phase (lower) of model A(a) and model B(b). Symbols with error bars are observed values and solid lines are calculated values. The models used in the calculation are also shown in the right hand side.

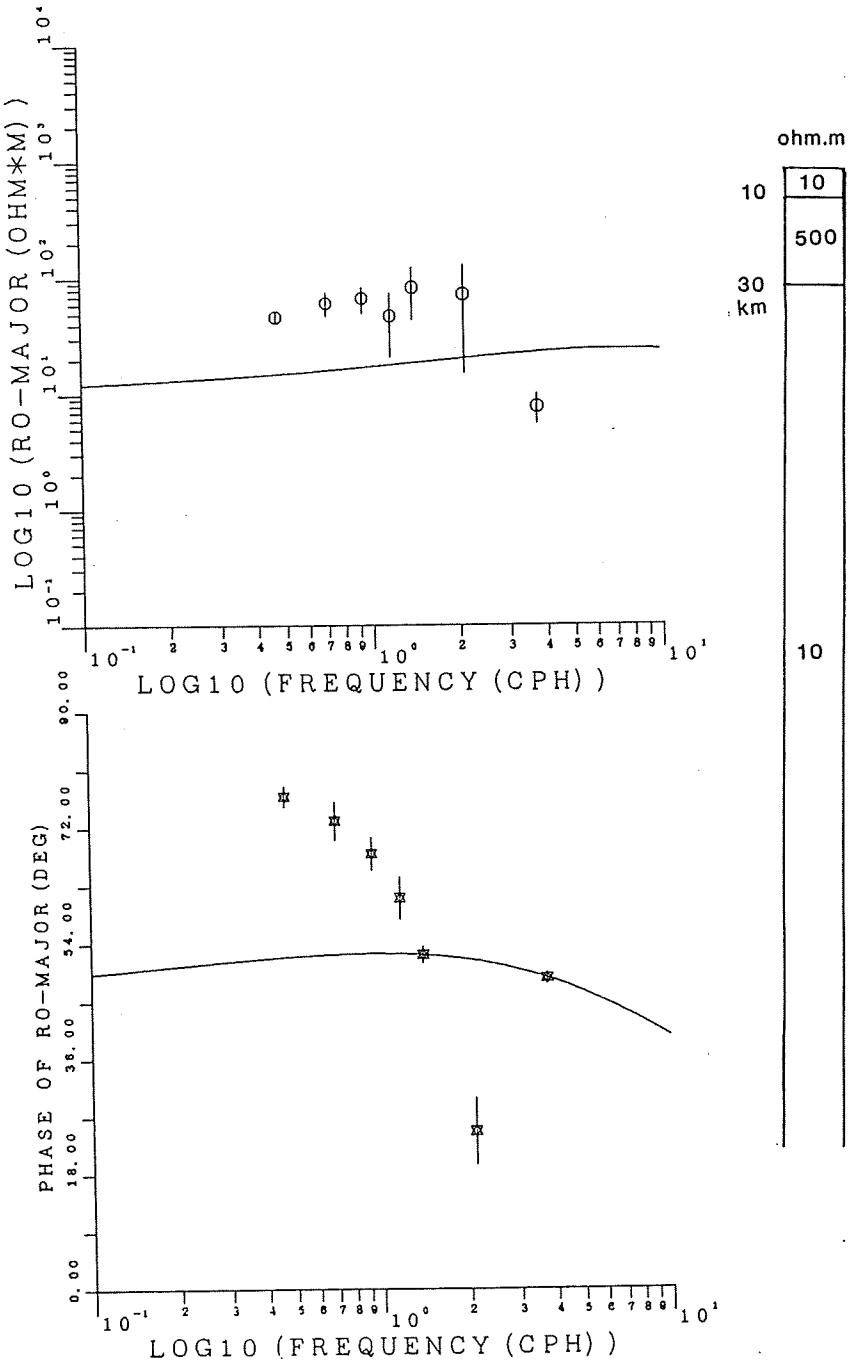

Fig. 8(b) (continued)

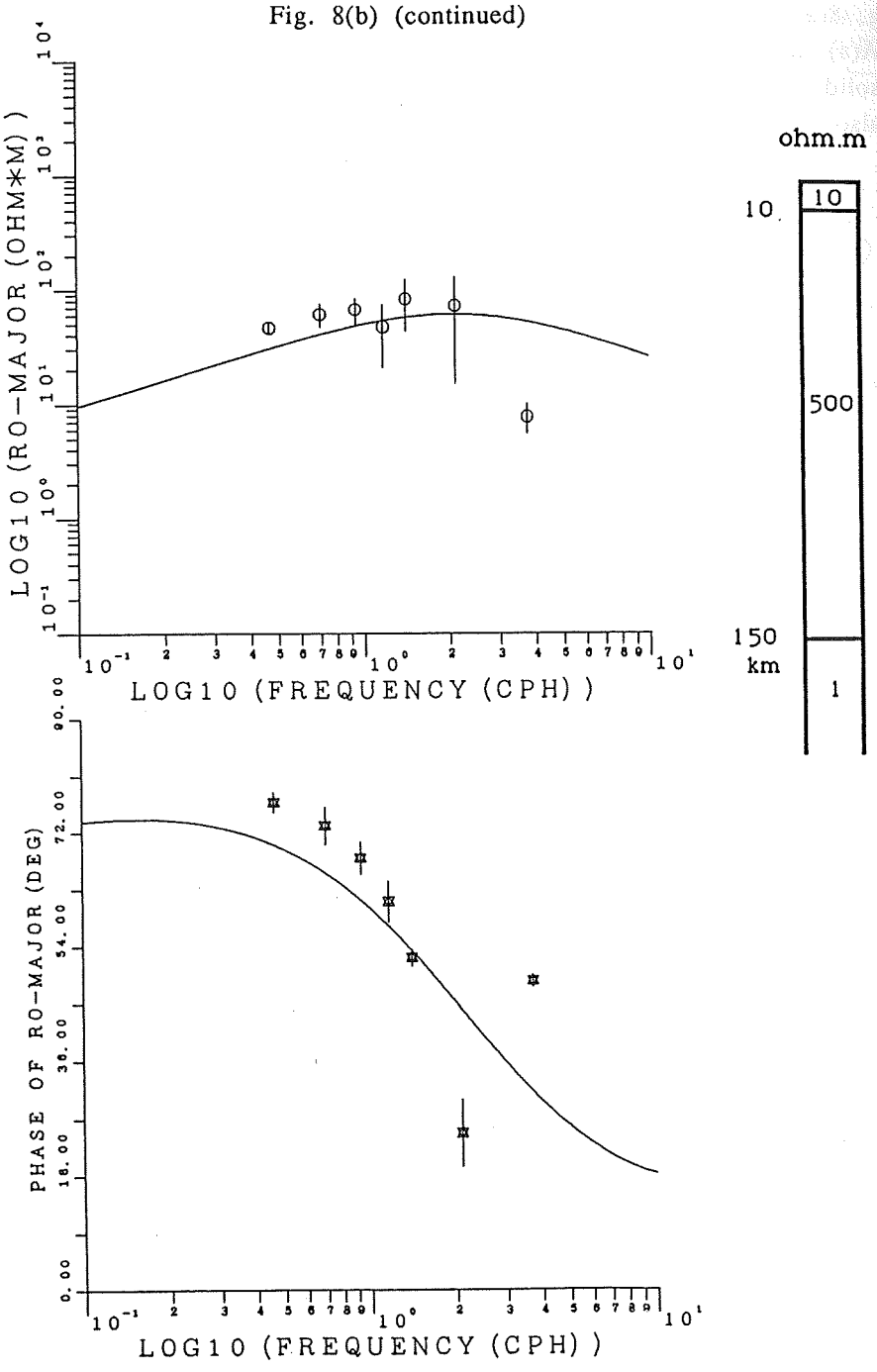

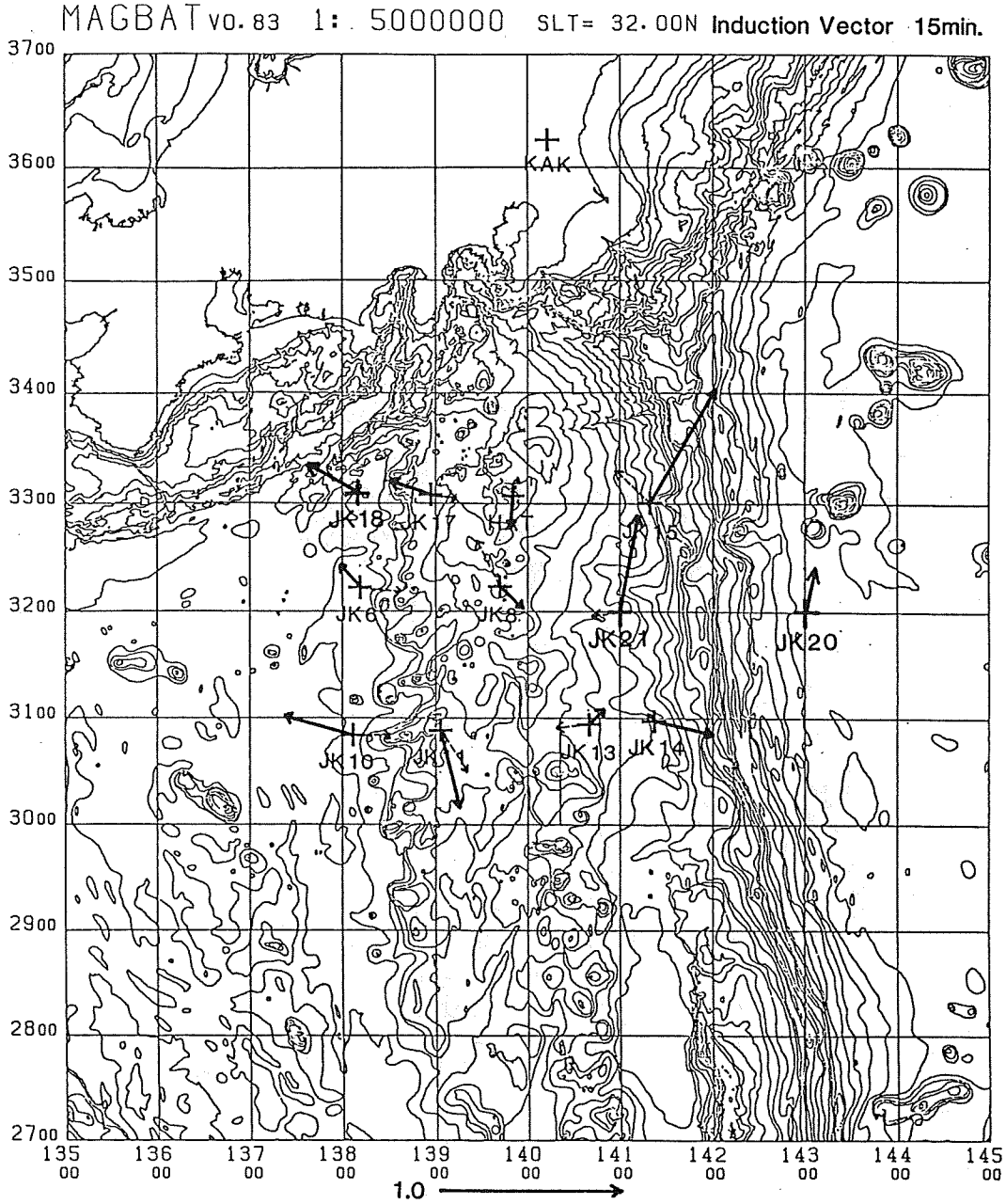

Fig. 9(a)-(d) Induction vectors for the period of 15 min (a), 30 min (b), 60 min (c) and 120 min (d). Arrows are plotted in the same manner as Fig. 1.

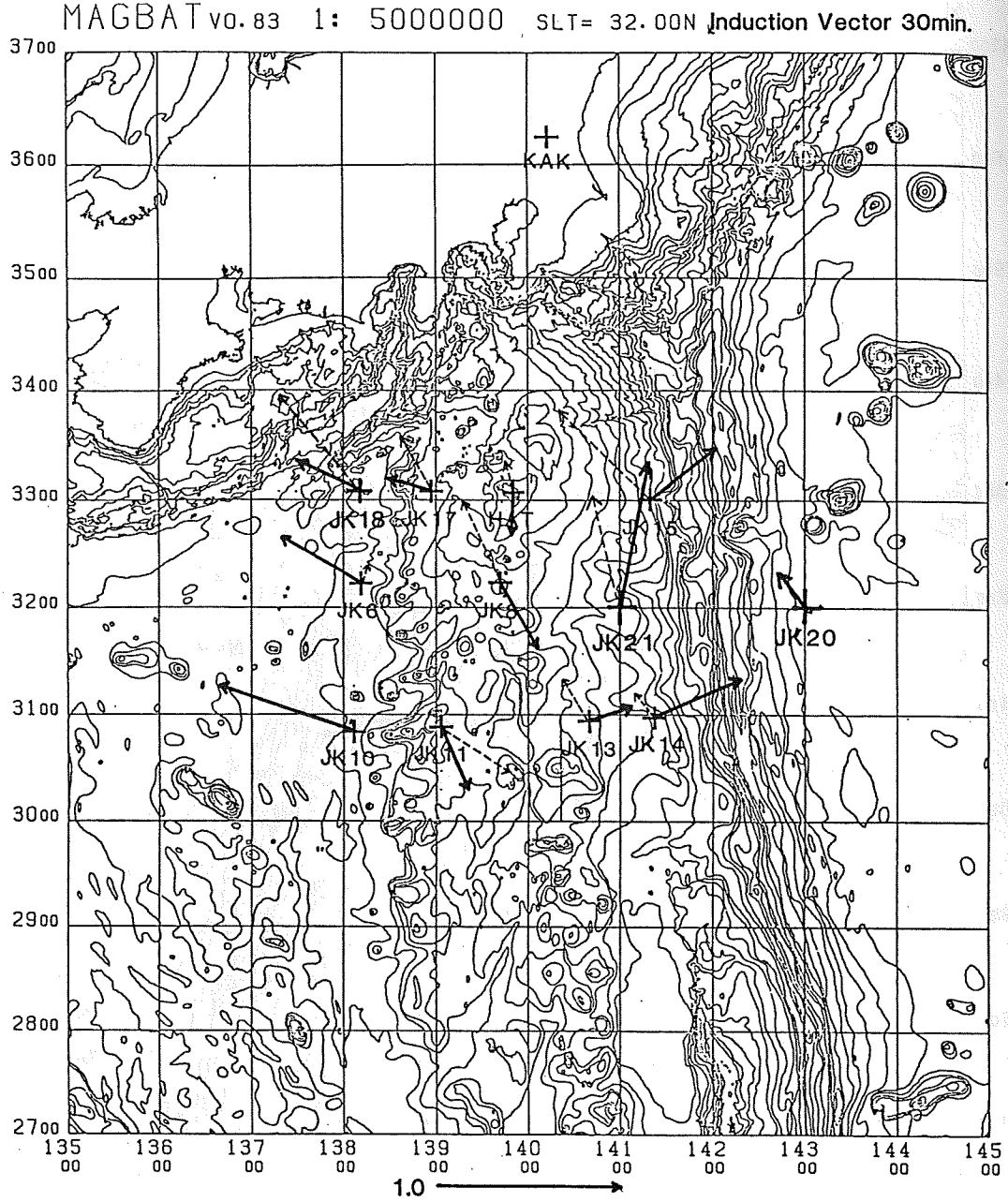

Fig. 9(b) (continued)

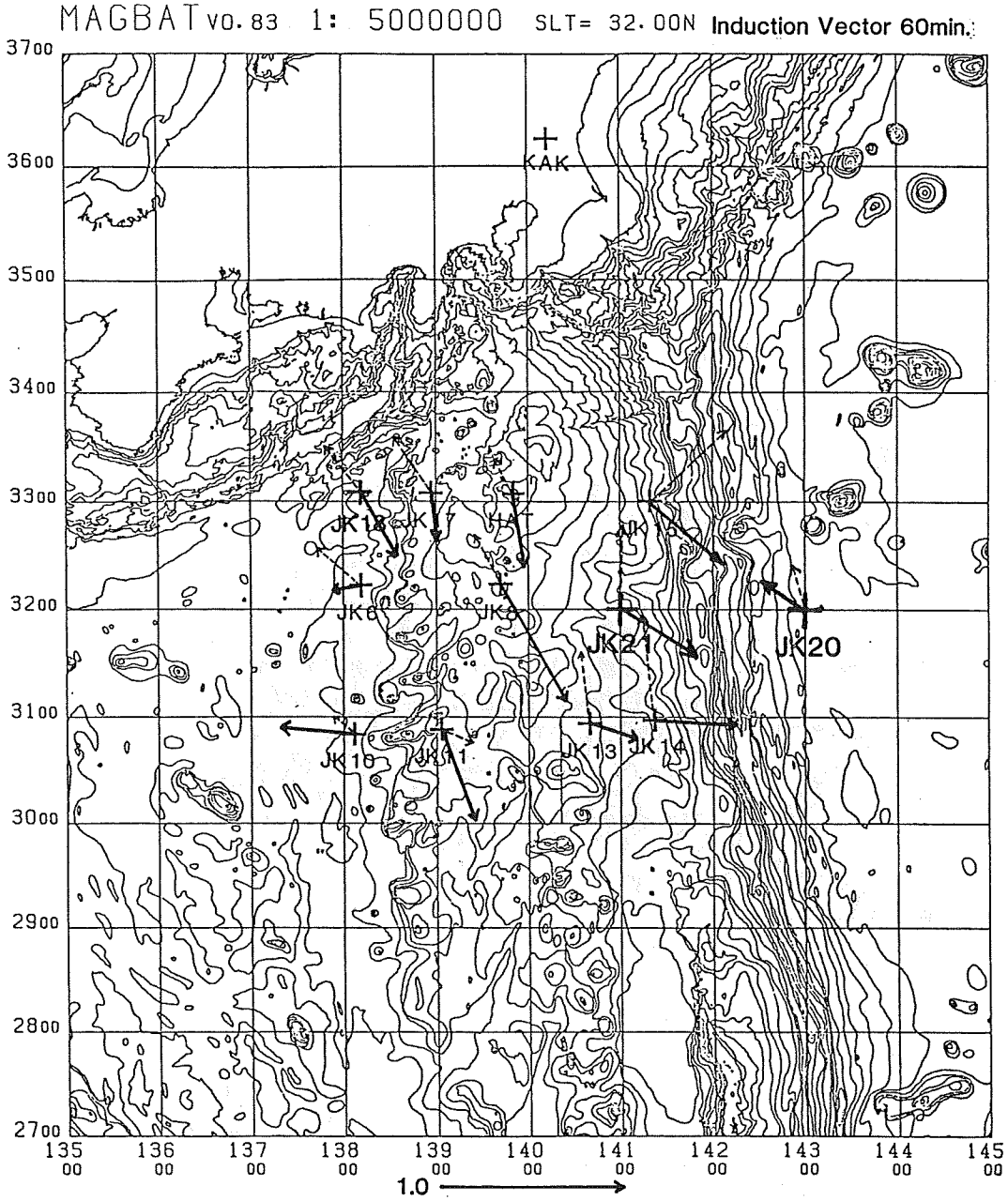

Fig. 9(c) (continued)

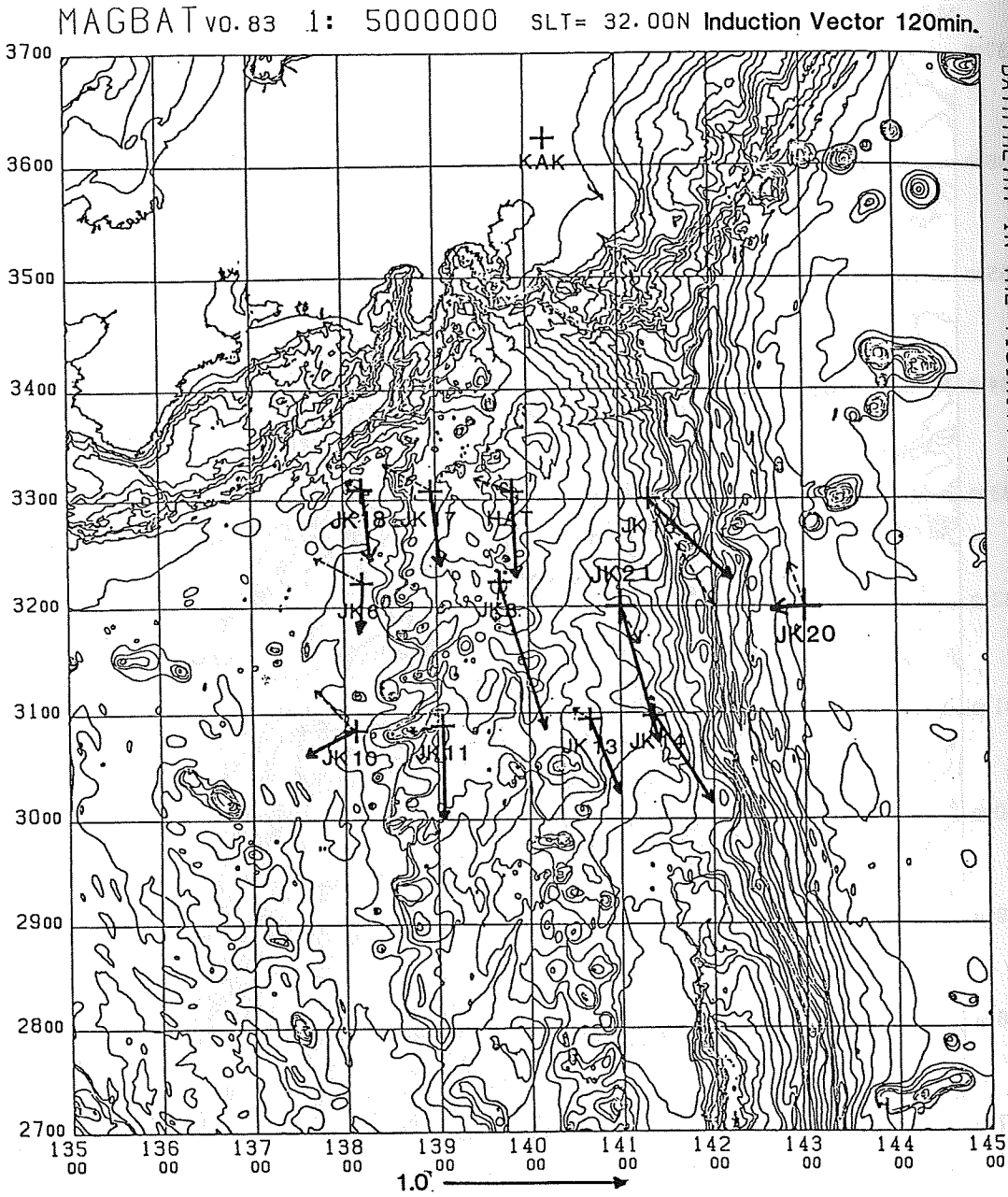

Fig. 9(d) (continued)